Journal of Membrane Science 438 (2013) 77–82

Contents lists available at SciVerse ScienceDirect

Journal of Membrane Science

journal homepage: www.elsevier.com/locate/memsci

Solidification characteristics of polymer solution during polyvinylidene fluoride membrane preparation by nonsolvent-induced phase separation

Toru Ishigami, Keisuke Nakatsuka, Yoshikage Ohmukai, Eiji Kamio, Tatsuo Maruyama, Hideto Matsuyama *

Center for Membrane and Film Technology, Department of Chemical Science and Engineering, Kobe University, 1-1 Rokkodai, Nada-ku, Kobe 657-8501, Japan

ARTICLE INFO

Article history:
Received 12 January 2013
Received in revised form
4 March 2013
Accepted 7 March 2013
Available online 22 March 2013

Keywords:
Solidification rate
Membrane preparation process
Nonsolvent-induced phase separation
Polyvinylidene fluoride

ABSTRACT

We investigated the solidification rate of polyvinylidene fluoride (PVDF) membranes during preparation by the nonsolvent-induced phase separation (NIPS) method. A new apparatus for quantitatively measuring membrane stiffness during phase separation was developed. In this apparatus, a polymer solution placed on a stage moves upward and the surface of the polymer solution contacts a sphere attached to the top of a needle. The displacement of a blade spring attached to the needle is then measured by a laser displacement sensor and converted to the surface repulsive force of the polymer solution. The effects of polymer concentration, composition of coagulant, molecular weight of polymer, and addition of hydrophilic additives were investigated. The solidification rate increases with increasing polymer concentration and molecular weight and decreases with the addition of solvent to the coagulation bath. The addition of hydrophilic additives causes rapid uptake of nonsolvent into the polymer solution and had the largest effect on solidification rate. Based on these results, two correlation groups between the solidification rate of the polymer solution and the mechanical strength of the ultimate membrane were identified. This is the first work to directly and quantitatively measure the solidification rate during nonsolvent-induced phase separation.

1. Introduction

Porous polymer membranes are widely applied in water treatment because of their efficiency in removing particles and microorganisms. The nonsolvent-induced phase separation (NIPS) method is one of the most important and common methods used to prepare porous polymer membranes for microfiltration and ultrafiltration. A polymer solution is simply immersed into a coagulation bath, which consists of a nonsolvent and the polymer solution then solidifies through exchange of the solvent and nonsolvent. An asymmetric membrane with a dense and thin skin layer can be easily prepared and the morphology can be controlled. Thus, NIPS enables high water permeability and preparation of a wide range of membrane morphology. Many studies of porous polymer membranes have focused on the prevention of fouling and improvement of membrane performance such as solute rejection and water permeability, which directly affect the efficiency of water treatment process. However, very few studies [1] have reported the solidification behavior of a polymer solution during the phase separation process, which significantly affects the industrial manufacturing process. Understanding the solidification behavior of polymer solution allows one to optimize the take-up speed of hollow fiber membranes and the design of the coagulation bath and rollers. Furthermore, the spinning of hollow fiber membranes is significantly influenced by the solidification of polymer solution during the NIPS process, because the solidification rate in this process is low. Bonyadi et al. [2] and Yin et al. [3] indicated that the solidification rate affects the morphology of fabricated hollow fiber membranes. Thus, it is important to understand the solidification behavior of polymer solution during the NIPS process.

Many researchers have investigated the phase equilibrium and kinetics of the NIPS process, including the mass transfer between solvent and nonsolvent and the phase separation rate, which may relate to the solidification of the polymer solution. Based on the Flory–Huggins theory [4], phase diagrams of the NIPS method have been constructed [5,6]. Cohen et al. [7], Reuvers et al. [8] and Tsay et al. [9] developed mass transfer models between solvent and nonsolvent during the phase separation process. A number of researchers investigated the effects of polymer concentration [5,10], coagulation temperature [11], addition of solvent to the coagulation bath [12], and polymer dissolution temperature [13] on membrane morphology. In addition, Guillen et al. [14] reported that the factors that affect the rate of liquid–liquid and solid–liquid demixing and polymer precipitation determine the ultimate

* Corresponding author. Tel./fax: +81 78 803 6180.
E-mail address: matuyama@kobe-u.ac.jp (H. Matsuyama).

0376-7388/$ - see front matter © 2013 Elsevier B.V. All rights reserved.
http://dx.doi.org/10.1016/j.memsci.2013.03.011

physical morphology of membranes. Furthermore, Sukitpaneenit et al. [15] discussed the relationship between elongation viscosity of the dope solution, the crystallinity and size of spherulitic globules in the morphology and the mechanical properties of fabricated membranes. However, these investigations did not study the dynamic stiffness during the phase separation but rather the ultimate mechanical strength. Several research groups studied the kinetics of the NIPS process through the light scattering method. This method readily provides information about the dynamic structure growth through phase separation. The effects of the additives on the dope solution [16,17] and the composition of the coagulation bath [18] were investigated. However, these studies investigated only the phase separation rate. To our knowledge, the solidification behavior of polymer solutions and dynamic mechanical properties during the NIPS process have been still not been described.

The aim of this study was to investigate the solidification characteristics of polymer solutions during the NIPS process. We developed a new apparatus to directly and quantitatively measure membrane stiffness during phase separation. The solidification rate of a polyvinylidene fluoride (PVDF) solution was then analyzed using this apparatus. In addition, the effect of several parameters that strongly affect the phase separation, such as the polymer concentration, composition of the coagulation bath, molecular weight of the polymer and types of additive to the polymer solution, were investigated. This represents the first step towards achieving a fundamental understanding of the solidification characteristics of polymer solutions during the NIPS process.

2. Experimental

2.1. Materials

For membrane preparation, PVDF of various molecular weights, namely M_w=136,000 (Solef 6008; Solvay Advanced Polymers Co.), 176,000 (Solef 1010; Solvay Advanced Polymers Co.), and 271,000 (Solef 1015; Solvay Advanced Polymers Co.) were used as polymer; dimethyl acetamide (DMAc, Wako Pure Chemical Industries, Osaka, Japan), as the solvent; polyvinylpyrrolidone (PVP, M_w=40,000, Tokyo Kasei Kogyo Co., Tokyo, Japan) and polyethylene glycol (PEG, M_w=6000, Wako Pure Chemical Industries), as additives. Water and a mixture of water and DMAc were used as coagulants. These materials were used without further purification.

2.2. Membrane stiffness measurement

Fig. 1 shows a diagram of the stiffness measurement apparatus. A sample of homogeneous PVDF solution was placed into a washer of thickness 2.5 mm on a petri dish and then placed onto the movable stage. 12 mL of nonsolvent was poured into the petri dish to induce phase separation. The stage was moved upward at 50 μm s^{-1} and the surface of the polymer solution during phase separation contacted a sphere attached to the top of a needle. The moving speed of the stage affects the measurement. When the moving speed is so high, the blade spring and the displacement sensor detect not only the surface stiffness of the polymer solution, but also the stiffness of inside of the polymer solution. The moving speed of the stage to 50 μm s^{-1} is properly adjusted that the apparatus detects the surface stiffness. The membrane stiffness was measured by contact between the polymer solution and the needle at arbitrary times during phase separation by adjusting the start time of the phase separation and the stage movement. The displacement of a blade spring attached to the needle, measured by a laser displacement sensor, was converted to the surface repulsive force of the polymer solution. The needle displacement was plotted against the displacement of the stage. To evaluate the membrane stiffness during phase separation, we used the gradient of the needle displacement against the stage displacement, as explained in Section 3.1.

2.3. Characterization of membrane and polymer solution

The membrane morphologies were examined under a scanning electron microscope (SEM, JSF-7500F; JEOL, Tokyo, Japan). To obtain dry membranes, the membranes were placed in a freeze dryer (FD-1000, EYELA, Tokyo, Japan) for 15 h. The dry membranes were fractured in liquid nitrogen and sputtered with Pt/Pd. The SEM images for membranes were obtained at an accelerating voltage of 15 kV. The viscosity of polymer solutions was measured at 25 °C using a viscometer (TVB-10, Toki Sangyo Co. Tokyo, Japan). To obtain the ultimate membrane strength, the tensile strength was measured with a tensile tester (AGS-J, Shimadzu Co. Kyoto, Japan). The membrane was fixed vertically between two pairs of tweezers and then extended at a constant elongation rate of 50 mm min^{-1} until it was broken.

3. Results and discussion

3.1. Validation of membrane stiffness measurement

To verify the membrane stiffness measurement, we first measured the stiffness of rubber sheets having 10° of hardness according to Japanese Industrial Standards (JIS K 6253). Fig. 2 (a) shows the relationship between the stage and spring displacement. The spring displacements are zero until around 200 μm of stage displacement, showing that the needle did not contact the rubber sheet until this point. Thereafter, the spring displacement continuously increases as a function of the stage displacement.

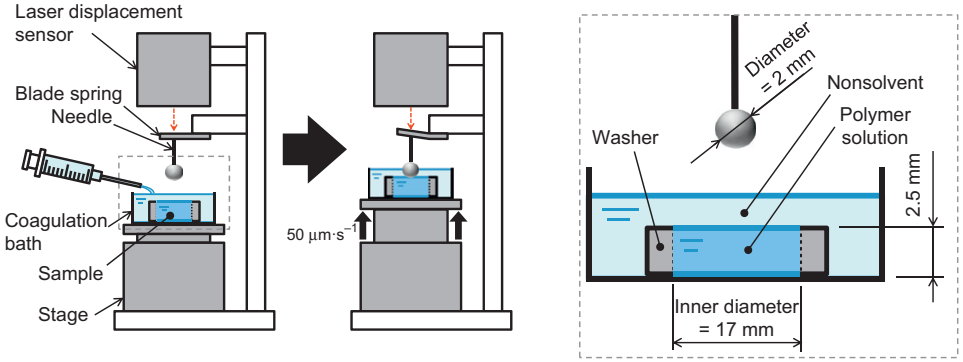

Fig. 1. Diagram of stiffness measurement apparatus.

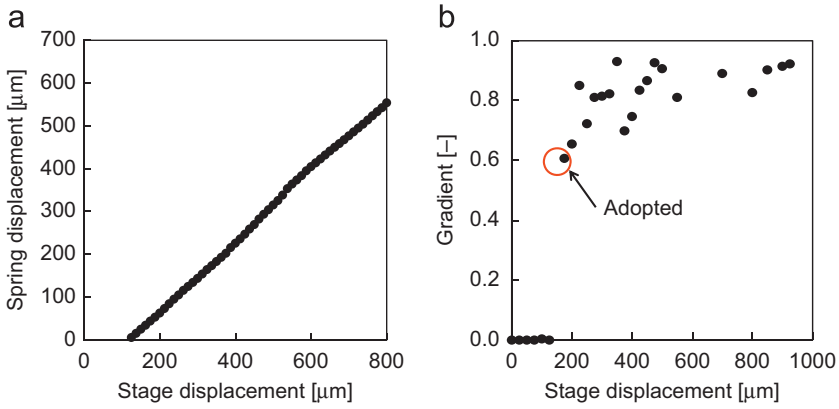

Fig. 2. Relationship between (a) spring displacement and stage displacement; and (b) gradient of spring displacement and stage displacement in the case of a rubber sheet hardness of 10°.

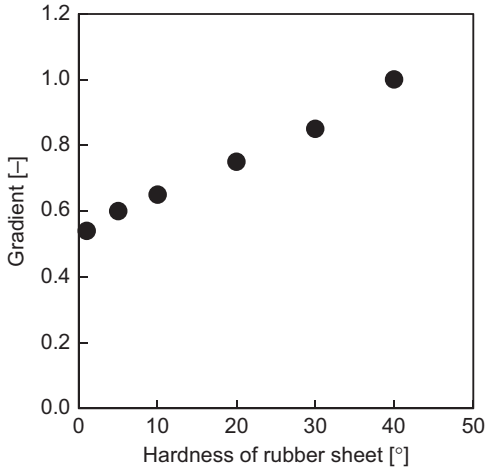

Fig. 3. Comparison of gradients for various rubber sheet hardnesses.

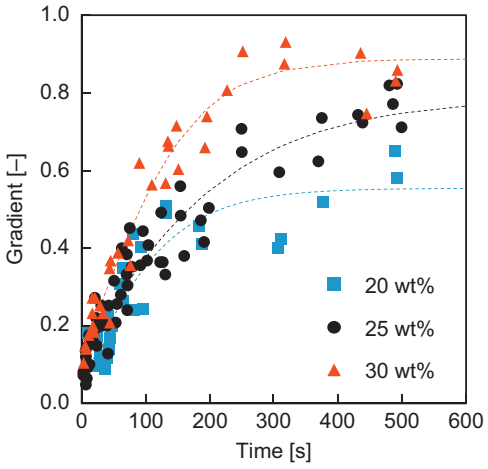

Fig. 4. Time variations in gradient with different polymer concentrations. Dot lines show the experimental tendencies.

The surface repulsive force is a product of the spring displacement and the spring constant. We adopted the gradient of the spring displacement over the stage displacement as a measure of the stiffness of a sample. The gradient was calculated by a forward Euler method. The gradient of the spring displacement over the stage displacement of 10° is shown instead of the spring displacement in Fig. 2(b). The gradient is initially zero, and then rises sharply as the needle contacts the rubber sheet. The gradient continuously increases after contacting, because the contact area between the sphere and rubber sheet increases with time. When this gradient reaches unity, the stage displacement is equal to the needle displacement, which occurs when the sample is sufficiently hard. The gradients were less than unity under the experimental conditions used herein. To minimize the effect of the increasing contact area, we used the gradient at the point where the needle contacts the rubber sheet as the stiffness of each sample. Fig. 3 shows the gradient data obtained for rubber sheets having 1, 5, 10, 20, 30 and 40° of hardness. The gradient clearly increases with increasing rubber sheet hardness. From these results, we confirm that the stiffness can be evaluated using our measurement method.

3.2. Effect of polymer concentration

The effects of polymer concentration in solution on solidification rate were investigated. The polymer concentration was changed in three steps; 20, 25 and 30 wt%. The molecular weight

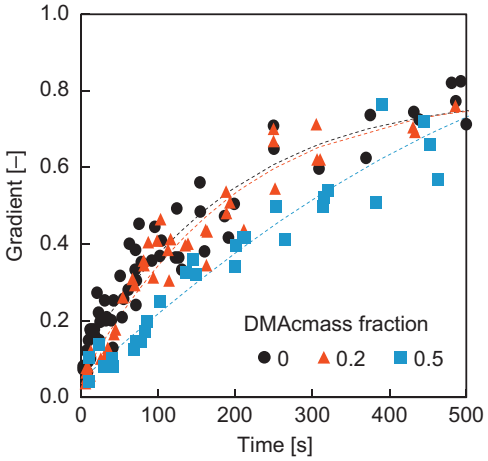

Fig. 5. Time variations in gradient with different compositions of the coagulation bath.

of PVDF was 136,000. The polymer solution contained no additives and water was used as the coagulation bath.

Fig. 4 shows the time variations of gradients. In all cases, the gradients increased with time because of induced phase separation. The gradient also increased with increasing polymer concentration, showing that the solidification rate of the polymer

solution increased with polymer concentration. Previous studies [5,10] explained that varying the initial polymer concentration changes the path to phase separation and the cloud point moves to the lower nonsolvent concentration region in the ternary phase diagram as polymer concentration increases. Thus, the higher polymer concentration brought about a high phase separation rate, which results in a higher solidification rate.

3.3. Effect of composition in the coagulation bath

The effects of solvent composition in the coagulation bath on solidification behavior were investigated. A mixture of water and DMAc was used as the coagulant. The mass fraction of DMAc in the coagulant bath was changed in three steps; 0, 0.2 and 0.5. The polymer concentration without additives was set to 25 wt% and the molecular weight of PVDF was 136,000.

Fig. 5 shows the time variations of gradients. The gradient decreases with increasing DMAc mass fraction in the coagulation bath, indicating that the solidification rate is lowered by the addition of DMAc to the coagulation bath. The mass transfer rate between the solvent in the polymer solution and coagulant decreases and the demixing changes from instantaneous to delayed with an increasing solvent fraction in the coagulant [19].

Table 1
PVDF solution viscosities with different molecular weights.

Molecular weight	Solution viscosity (Pa s)
136,000	2.7
176,000	7.1
271,000	67.1

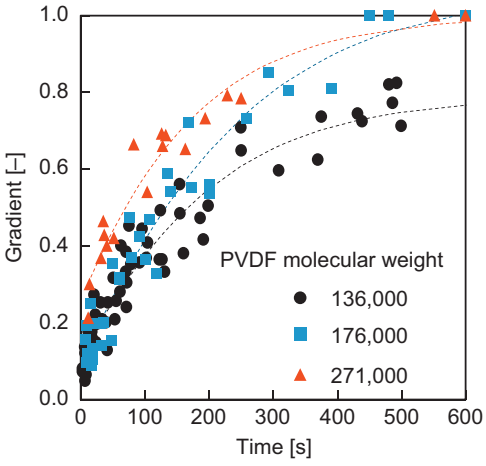

Fig. 6. Time variations in gradient with different PVDF molecular weights.

The delayed demixing process may bring about the low solidification rate. However, the solidification rate difference reduces with time, indicating that the coagulation bath composition has less effect on the final membrane stiffness than the polymer concentration. The final membrane stiffness may thus be most strongly affected by the polymer concentration.

3.4. Effect of molecular weight

The polymer molecular weight was changed in three steps; 136,000, 176,000 and 271,000. Varying the molecular weight also changes the viscosity of the polymer solution. Therefore, the effects of the polymer solution viscosity on the solidification behavior were examined. The solution viscosities are shown in Table 1. The solution viscosity increases sharply with increasing molecular weight. In this experiment, water was used as the coagulant and the polymer concentration without additives was set to 25 wt%.

The gradient increases with increasing molecular weight, as shown in Fig. 6, indicating that the solidification rate increases with increasing solution viscosity, despite the associated decrease in solvent–nonsolvent diffusion [20]. Varying solution viscosity may therefore change the membrane morphology. Fig. 7 shows SEM images of cross-sections near the outer surfaces of the resultant membranes. In the case of the lowest molecular weight, large-sized finger-like macrovoid structures can be observed, as shown in Fig. 7(a), indicating that instantaneous demixing occurs due to the low solution viscosity. The sizes of the macrovoids decrease with increasing molecular weight (Fig. 7(a) and (b)). In the case of the highest molecular weight, no macrovoids can be seen and a dense top layer is instead observed, as seen in Fig. 7(c). These differing membrane morphologies may affect the differences in membrane stiffness during phase separation.

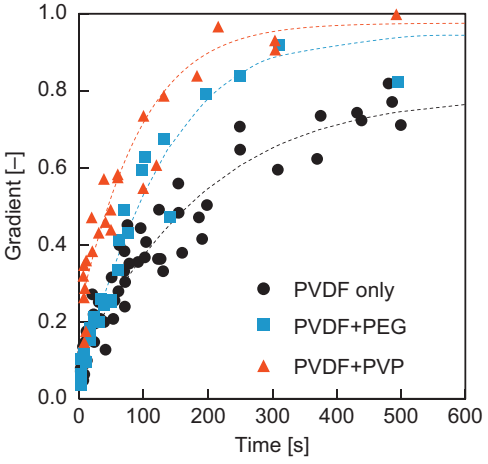

Fig. 8. Time variations in gradient without and with addition of PEG and PVP to polymer solution.

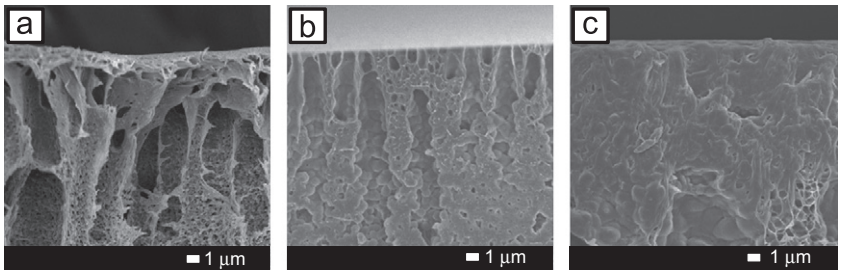

Fig. 7. Cross-sectional SEM images near the outer surfaces with different PVDF molecular weights. (a) M_w=136,000; (b) M_w=176,000; and (c) M_w=271,000.

3.5. Effect of additives

The effects of addition of PEG and PVP, which are hydrophilic additives often used as viscosity-increasing agents for membrane fabrication, were investigated. PVDF and the additive concentration were set to 25 wt% and 5 wt%, respectively. Water was used as the coagulant.

Fig. 8 shows the time variations of gradients. The gradients significantly increase with both PEG and PVP addition. Furthermore, the gradient for PVP addition is higher than that for PEG addition. Many researchers studied the role of additives on membrane preparation via the NIPS method [15,21,22]. Addition of PEG and PVP to the polymer solution can significantly improve the membrane properties but it makes the solvent–nonsolvent system more complex. To elucidate the factors influencing solidification, the resultant membrane morphologies were observed.

Fig. 9 shows SEM images of cross-sections and the outer surfaces of the prepared membranes. As can be seen in the cross-sectional images, the depths of finger-like macrovoids clearly increase with additives (Fig. 9(b1) and (c1)) compared with those without additives (Fig. 9(a1)). This indicates that the additives enhance the uptake of nonsolvent into the polymer solution. In addition, the macrovoids with PVP addition are larger than those with PEG addition. On the outer membrane surface, an interconnected-cellular structure can be observed in the case of additives to the polymer solution (Fig. 9(b2) and (c2)), while a spherulite globule structure is obtained without additives (Fig. 9 (a2)). This is because the instantaneous demixing in the presence of additives suppresses the formation of the spherulite globule structure. Sukitpaneet et al. [15] reported that membranes with a spherulitic globule morphology have a lower mechanical strength than those with interconnected-cellular type morphology and that the mechanical strength is hardly affected by the macrovoid size. Therefore, the enhanced phase separation rate and transformation to interconnected-cellular morphology due to the presence of additives can increase the solidification rate.

The addition of additives to the polymer solution enhances the uptake of nonsolvent into the polymer solution because of the latter's increased hydrophilicity. Higher nonsolvent uptake rates due to an increased miscibility between the solvent and the nonsolvent also cause macrovoid growth, as shown in Fig. 9(b1) and (c1). For this reason, the addition of additives significantly accelerated the solidification rate.

3.6. Relationship between solidification rate and tensile stress of the membrane

We summarize below the effects of the polymer concentration, molecular weight of polymer and additives on the solidification rate. The solidification rates under each condition were evaluated by the linear interpolation of gradients during the period from 0 s to 100 s in Figs. 4, 6 and 8. Fig. 10 shows the relationship between the solidification rate of the polymer solutions and the tensile stress of the resultant membranes. Overall, membranes prepared under conditions of a higher solidification rate showed a higher tensile stress. However, there are two groups that show correlations. Increasing both polymer concentration and polymer molecular weight brought about similar correlation trends. However, the data in the cases of the addition of hydrophilic additives deviated from this correlation. Additives significantly enhanced the initial solidification rate because of the increasing hydrophilicity of the polymer solutions, as described above. However, the addition of such hydrophilic additives resulted in membranes with

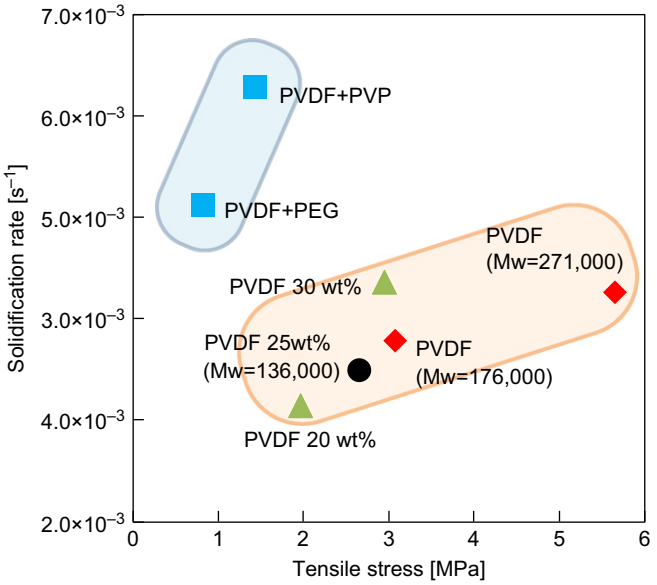

Fig. 10. Relationship between the solidification rate of the polymer solutions and ultimate tensile stress and comparison of factors that influenced the solidification rate. Black circle, raw PVDF only (control); green triangles, effect of polymer concentration; red diamonds, effect of molecular weight; blue squares, effect of additive. (For interpretation of the references to color in this figure caption, the reader is referred to the web version of this article.)

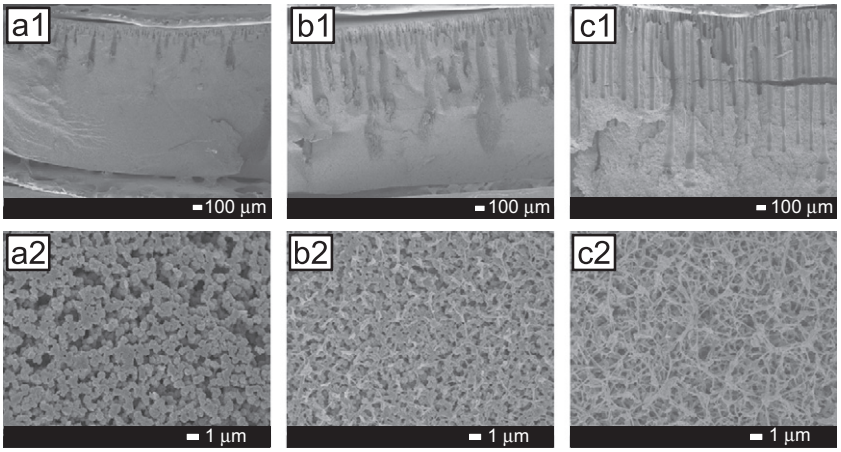

Fig. 9. SEM images of membranes with a, no additives; b, PEG; c, PVP. 1, cross-section; 2, outer surface.

large finger-like macrovoids, as shown in Fig. 9(b1) and (c1). Thus, the tensile stress of the final membranes was not increased to the same extent as without additives.

4. Conclusions

In this study, we developed a new apparatus for directly measuring membrane stiffness and quantitatively analyzed the solidification behavior of polymer solutions during nonsolvent phase separation. The effects of polymer concentration, composition of the coagulant, molecular weight of polymer and additives were investigated using the apparatus. The following conclusions were drawn from the results:

1. Solidification is affected by polymer concentration, composition of coagulant, solution viscosity and addition of hydrophilic additives.
2. Addition of hydrophilic additives to the polymer solution significantly accelerates the solidification rate because the uptake of water into the polymer solution is enhanced.
3. There are two correlation groups between the solidification rate of polymer solution and the ultimate membrane strength.

To the best our knowledge, this is the first work to directly and quantitatively measure the solidification rate of polymer solutions during nonsolvent-induced phase separation. The findings from this study will be useful for the industrial manufacture of porous polymer membranes by the NIPS method.

References

[1] S. Liu, C. Zhou, W. Yu, Phase separation and structure control in ultra-high molecular weight polyethylene microporous membrane, J. Membr. Sci. 379 (2011) 268.
[2] S. Bonyadi, T.S. Chung, W.B. Krantz, Investigation of corrugation phenomenon in the inner contour of hollow fibers during the non-solvent induced phase-separation process, J. Membr. Sci. 299 (2007) 200.
[3] J. Yin, N. Coutris, Y. Huang, Experimental investigation of aligned groove formation on the inner surface of polyacrylonitrile hollow fiber membrane, J. Membr. Sci. 394 (2012) 57.
[4] P.J. Flory, Principles of Polymer Chemistry, 10th ed., Cornell Univ. Pr., Ithaca, New York, 672.
[5] H. Strathmann, K. Kock, The formation mechanism of phase inversion membranes, Desalination 21 (1977) 241.
[6] J.G. Wijmans, J. Kant, M.H.V. MulderC.A. Smolders, Phase separation phenomena in solutions of polysulfone in mixtures of a solvent and a nonsolvent: relationship with membrane formation, Polymer 26 (1985) 1539.
[7] C. Cohen, G.B. Tanny, S. Prager, Diffusion-controlled formation of porous structures in ternary polymer systems, J. Polym. Sci., Part B: Polym. Phys. 17 (1979) 477.
[8] A.J. Reuvers, J.W.A. VandenbergC.A. Smolders, Formation of membranes by means of immersion precipitation. 1. A model to describe mass-transfer during immersion precipitation, J. Membr. Sci. 34 (1987) 45.
[9] C.S. Tsay, A.J. McHugh, Mass-transfer modeling of asymmetric membrane formation by phase inversion, J. Polym. Sci., Part B: Polym. Phys. 28 (1990) 1327.
[10] H. Strathmann, K. Kock, P. Amar, R.W. Baker, Formation mechanism of asymmetric membranes, Desalination 16 (1975) 179.
[11] X. Wang, L. Zhang, D. Sun, Q. An, H. Chen, Formation mechanism and crystallization of poly(vinylidene fluoride) membrane via immersion precipitation method, Desalination 236 (2009) 170.
[12] K.Y. Chun, S.H. Jang, H.S. Kim, Y.W. Kim, H.S. Han, Y.I. Joe, Effects of solvent on the poreformation in asymmetric 6FDA–4,4′ODA polyimide membrane: terms of thermodynamics, precipitation kinetics, and physical factors, J. Membr. Sci. 169 (2000) 197.
[13] C.L. Li, D.M. Wang, A. Deratani, D. Quemener, D. Bouyer, J.Y. Lai, Insight into the preparation of poly(vinylidene fluoride) membranes by vapor-induced phase separation, J. Membr. Sci. 361 (2010) 154.
[14] G.R. Guillen, Y. Pan, M. Li, E.M.V. Hoek, Preparation and characterization of membranes formed by nonsolvent induced phase separation: a review, Ind. Eng. Chem. Res. 50 (2011) 3798.
[15] P. Sukitpaneenit, T.S. Chung, Molecular elucidation of morphology and mechanical properties of PVDF hollow fiber membranes from aspects of phase inversion, crystallization and rheology, J. Membr. Sci. 340 (2009) 192.
[16] J.H. Kim, K.H. Lee, Effect of PEG additive on membrane formation by phase inversion, J. Membr. Sci. 138 (1998) 153.
[17] H. Matsuyama, T. Maki, M. Teramoto, K. Kobayashi, Effect of PVP additive on porous polysulfone membrane formation by immersion precipitation method, Sep. Sci. Technol. 38 (2003) 3449.
[18] A.J. Reuvers, C.A. Smolders, Formation of membranes by means of immersion precipitation. Part II. The mechanism of formation of membranes prepared from the system cellulose acetate-acetone-water, J. Membr. Sci. 34 (1987) 67.
[19] M. Mulder, Basic Principles of Membrane Technology, Kluwer Academic Publishers, Dordrecht, The Netherlands, 2003.
[20] Q.Z. Zheng, P. Wang, Y.N. Yang, Rheological and thermodynamic variation in polysulfone solution by PEG introduction and its effect on kinetics of membrane formation via phase-inversion process, J. Membr. Sci. 279 (2006) 230.
[21] R.M. Boom, I.M. Wienk, T. Vandenboomgaard, C.A. Smolders, Microstructures in phase inversion membranes. 2. The role of a polymeric additive, J. Membr. Sci. 73 (1992) 277.
[22] J.H. Kim, K.H. Lee, Effect of PEG additive on membrane formation by phase inversion, J. Membr. Sci. 138 (1998) 153.